

# A Molecular and Structural Mechanism for G Protein-mediated Microtubule Destabilization<sup>\*S</sup>

Received for publication, October 20, 2010, and in revised form, November 16, 2010. Published, JBC Papers in Press, November 26, 2010, DOI 10.1074/jbc.M110.196436

Rahul H. Davé<sup>†S1</sup>, Witchuda Saengsawang<sup>†1</sup>, Manu Lopus<sup>¶</sup>, Sonya Davé<sup>||</sup>, Leslie Wilson<sup>¶</sup>, and Mark M. Rasenick<sup>†\*\*2</sup>

From the <sup>†</sup>Department of Physiology and Biophysics, the <sup>\*\*</sup>Department of Psychiatry, and the <sup>S</sup>Medical Scientist Training Program, University of Illinois, Chicago, Illinois 60612, the <sup>¶</sup>Department of Molecular, Cellular, and Developmental Biology and the Neuroscience Research Institute, University of California, Santa Barbara, California 93106, and the <sup>||</sup>Department of Molecular Physiology and Biophysics, Vanderbilt University School of Medicine, Nashville, Tennessee 37212

The heterotrimeric, G protein-coupled receptor-associated G protein,  $G\alpha_s$ , binds tubulin with nanomolar affinity and disrupts microtubules in cells and *in vitro*. Here we determine that the activated form of  $G\alpha_s$  binds tubulin with a  $K_D$  of 100 nM, stimulates tubulin GTPase, and promotes microtubule dynamic instability. Moreover, the data reveal that the  $\alpha 3$ – $\beta 5$  region of  $G\alpha_s$  is a functionally important motif in the  $G\alpha_s$ -mediated microtubule destabilization. Indeed, peptides corresponding to that region of  $G\alpha_s$  mimic  $G\alpha_s$  protein in activating tubulin GTPase and increase microtubule dynamic instability. We have identified specific mutations in peptides or proteins that interfere with this process. The data allow for a model of the  $G\alpha_s$ /tubulin interface in which  $G\alpha_s$  binds to the microtubule plus-end and activates the intrinsic tubulin GTPase. This model illuminates both the role of tubulin as an “effector” (e.g. adenylyl cyclase) for  $G\alpha_s$  and the role of  $G\alpha_s$  as a GTPase activator for tubulin. Given the ability of  $G\alpha_s$  to translocate intracellularly in response to agonist activation,  $G\alpha_s$  may play a role in hormone- or neurotransmitter-induced regulation of cellular morphology.

Microtubules are dynamic polymers composed of  $\alpha$ - $\beta$  tubulin dimers with kinetically and structurally distinct plus- and minus-ends. Both subunits contain guanine nucleotides. GTP, in the  $\alpha$  subunit, is non-exchangeable and non-hydrolyzable. However, GTP in the  $\beta$  subunit, which is exposed at the dynamic plus-ends, is exchangeable and hydrolyzable (it can exchange the GDP with GTP present in the reaction mixture or in the intracellular milieu). Microtubules assemble by the sequential addition of tubulin-GTP to the ends. Newly added tubulin-GTP catalyzes the hydrolysis of GTP to GDP, creating a very short GTP (or GDP- $P_i$ )-tubulin “cap” at the ends and a core of GDP-tubulin (1). This cap at the microtubule tip stabilizes the entire microtubule and prevents rapid

disassembly. Loss of the stabilizing cap results in an abrupt switching of an end from growth to shortening, called a catastrophe.

Regulated assembly and disassembly of microtubules play pivotal roles in the genesis, maintenance, and functioning of the nervous system (2). In particular, dynamic microtubules are located in regions of high neuronal plasticity, such as the tips of growing neurites and immature dendritic spines (3–5). How the dynamics of microtubules at their plus-ends is regulated to enable them to perform their diverse cellular functions in the nervous system and elsewhere is a central question in cell biology.

Heterotrimeric guanine nucleotide-binding proteins (G proteins) transduce extracellular neurotransmitter (or hormone) stimuli into intracellular signaling cascades. In response to hormone or neurotransmitter activation of G protein-coupled receptors, the  $G\alpha$  and  $G\beta\gamma$  subunits functionally dissociate, and the inactive  $G\alpha$  exchanges its GDP for GTP, resulting in active  $G\alpha$ -GTP. Active  $G\alpha$  subunits exert intracellular effects by stimulating effectors, such as (in the case of  $G\alpha_s$ ) adenylyl cyclase, which generates cyclic AMP from ATP. In addition to stimulating adenylyl cyclase, G proteins also directly affect microtubule stability (6–8). For example, in cells, activation of  $G\alpha_s$  and the attendant increase in cAMP have been suggested to modulate microtubule dynamics and neurite outgrowth (6, 9). Moreover, active G proteins can promote neurite outgrowth independently of cAMP by directly binding to microtubules (6). Activation of G protein-coupled receptors by hormones or neurotransmitters evokes translocation of  $G\alpha_s$  from G protein-coupled receptors into lipid rafts (10).  $G\alpha_s$  then internalizes, and the intracellular  $G\alpha_s$  interacts with microtubules and destabilizes microtubules, leading to neurite outgrowth (6). Supporting this argument,  $G\alpha_s$  binds tubulin from rat brain extracts and binds with nanomolar affinity *in vitro* and co-immunoprecipitates tubulin from rat brains (11–13). In addition, *in vitro* studies have shown that  $G\alpha$  subunits increase microtubule dynamics, possibly by acting as a GTPase-activating protein (6, 8). It has been proposed that  $G\alpha$  binds to the plus-ends of microtubules and destroys the stabilizing GTP (GDP- $P_i$ ) cap, allowing for increased microtubule dynamics (6, 8). Recent modeling studies of tubulin- $G\alpha_s$  interactions support this possibility (13). Although the cellular effects of  $G\alpha_s$  activation on microtubules and neuronal outgrowth have been described (6), the molecu-

\* This work was supported, in whole or in part, by National Institutes of Health Grants NS 13560 (to M. L. and L. W.), T32-HL007692 (to R. H. D.), and MH 39595 (to W. S. and M. M. R.). This work was also supported by AbdulRazaq Al-Siddiqi.

<sup>S</sup> The on-line version of this article (available at <http://www.jbc.org>) contains supplemental Tables 1–3 and Figs. 1 and 2.

<sup>1</sup> Both authors contributed equally to this work.

<sup>2</sup> To whom correspondence should be addressed: Dept. of Physiology and Biophysics, College of Medicine, University of Illinois, 835 S. Wolcott, M/C 901, Chicago, IL 60612-7342. Tel.: 312-996-6641; Fax: 312-996-1414; E-mail: raz@uic.edu.

## Mechanism for $G\alpha_s$ -mediated Microtubule Destabilization

lar and structural mechanisms by which  $G\alpha_s$  destabilizes microtubules remain unclear.

The purpose of the current study was to elucidate the mechanism by which  $G\alpha_s$  increases dynamic instability and thus destabilizes microtubules. We show that active  $G\alpha_s$  increases microtubule dynamics in association with stimulation of tubulin GTPase activity. Further, using a combination of biochemical and computational approaches, we identify the  $\alpha 3$ – $\beta 5$  region as the functionally important structural motif in  $G\alpha_s$  that is involved in the G protein-mediated alteration of microtubule dynamics. In addition, we find that peptides derived from this motif mimic the effects of  $G\alpha_s$  on both tubulin GTPase and microtubule dynamics. These peptides or small molecules based on them may lead to novel therapeutic agents for promoting neuronal outgrowth and differentiation *in vivo*.

### EXPERIMENTAL PROCEDURES

**Materials**—His- $G\alpha_s^{WT}$  and His- $G\alpha_s^{Q227L}$  in pRSET plasmids were obtained from Dr. Tarun Patel (Loyola University, Maywood, IL). Peptides were custom synthesized by the University of Illinois Chicago Protein Research Laboratory. Peptide sequences are as follows: KQLQKDKQVYRATHR (peptide N), EDAEKDARVYRATVK (peptide GtN), LNLFKSIWNNRWLRT (peptide 3), LHLFNSICNHRFYFAT (peptide-Gt3), LHLFNSIWNNRWLRT (peptide M1), LNLFKSICNHRWLRT (peptide M2), LNLFKSIWNNRYFAT (peptide M3), LHLFNSIWNNRYFAT (peptide M5), and LNLFKSICNHRFYFAT (peptide M6). Radiochemicals were obtained from MP Biochemicals (Irvine, CA).

**Mutagenesis**—Mutagenesis was performed using the QuikChange kit (Stratagene, La Jolla, CA), following the manufacturer's protocol.  $G\alpha_s$ - $G\alpha_t$  chimeras were created (see supplemental Table 1) by mutating His- $G\alpha_s^{WT}$  in a pRSET plasmid, and final products were confirmed by DNA sequencing (UIC Research Resources Center) from both the 5'- and 3'-ends.

**Protein Purification**—Recombinant His- $G\alpha_s$  and mutated proteins were purified using previously published methods (14, 15). Induction conditions, optimized to maximize soluble protein expression, were as follows:  $G\alpha_s^{Q227L}$  (hereafter referred to as  $G\alpha_s^{QL}$ ), 20 h at 15 °C, 17 h at 25 °C;  $G\alpha_s^{GtLoop/Q227L}$  (hereafter referred to as  $G\alpha_s^{GtL/QL}$ ), 20 h at 25 °C. The function of  $G\alpha_s^{WT}$  was tested by assessing the change in tryptophan fluorescence of  $G\alpha_s$  in response to binding  $AlF_4^-$  (16).  $G\alpha_s$ -GDP was generated by incubating  $G\alpha_s^{WT}$  with 5 mM  $MgCl_2$  for 1 h at 37 °C.

Ovine and bovine tubulin were purified using two polymerization-depolymerization cycles followed by phosphocellulose chromatography and stored in PEM buffer (100 mM PIPES, 1 mM  $MgCl_2$ , 1 mM EDTA, pH 6.8) (17, 18). Tubulin was stored in liquid nitrogen until use. Bovine brain tubulin was used in dynamics and polymer mass assays, and ovine brain tubulin was used in all other experiments.

**Surface Plasmon Resonance (Biacore 1000)**—Quantitative analyses of peptide/protein-tubulin interactions were performed on a Biacore 1000 system (GE Healthcare). To determine  $G\alpha_s$ -tubulin affinity, tubulin was immobilized on a car-

boxymethyl dextran-coated CM5 BIAcore sensor chip, and  $G\alpha_s$  was allowed to bind. Tubulin was immobilized in HBS-P buffer, pH 7.4 (10 mM HEPES, 150 mM NaCl, and 0.005% (v/v) surfactant P-20) at a flow rate of 10  $\mu$ l/min on sensor chip CM5.

His- $G\alpha_s^{Q227L}$  or His- $G\alpha_s^{WT}$  was exchanged into Biacore buffer twice (10 mM HEPES, 150 mM NaCl, 0.005% P-20, pH 6.9) using protein desalting columns (7 kDa cut-off; Pierce). The  $G\alpha_s$  proteins or peptides were allowed to bind to immobilized tubulin at 25 °C (10 min for proteins; 100 s for peptides), followed by 15 min of dissociation at a 10  $\mu$ l/min flow rate in buffer. To achieve complete removal of bound  $G\alpha_s$ , flow cells were injected twice with a regeneration solution (0.5% Triton X-100 in 1 M NaCl in HBS-P buffer) for 15 s at 30  $\mu$ l/min, followed by an "extraclean" step after each regeneration. Regeneration conditions were optimized to maintain tubulin stability while removing most of the bound G protein or peptide. Each sample was injected into a reference flow cell to control for nonspecific binding. A buffer-only tube was run between every 2–3 tubes.

The final kinetic curves were obtained by first subtracting the blank condition and then subtracting the reference flow cell curves. The resulting curve was fit to a 1:1 Langmuir kinetic association model with drifting base line, per manufacturer's instructions. The calculated base-line drift was within the specifications of the instrument, and  $\chi^2$  values were <2.0. We used ovalbumin as the control. Ovalbumin did not detectably bind tubulin (1  $\mu$ M) under this condition. Statistical analyses were performed using BIAevaluation 4.1 and GraphPad Prism 4.0 software.

**Single Turnover Tubulin GTPase Activity Assay**—A single turnover GTPase activity assay was performed as described previously (19). Briefly, [ $\gamma$ - $^{32}P$ ]GTP (450 mCi/mol) was exchanged onto 2  $\mu$ M tubulin on ice (PEM buffer), and unbound [ $^{32}P$ ]GTP was removed using a desalting column (Pierce). 200 nM tubulin- $^{32}P$ GTP was incubated with the indicated G protein construct, and the released  $^{32}P$  was isolated using charcoal extraction and quantified by scintillation spectrometry (Beckman LS-6000 (Brea, CA) and Econosafe Scintillation Fluid (Research Products International, Mount Prospect, IL)).

**Microtubule Polymerization Assay**—Microtubule polymerization was performed using 15  $\mu$ M tubulin in G-PEM buffer (100 mM PIPES, 1 mM  $MgCl_2$ , 2 mM EDTA, 200  $\mu$ M GTP, pH 6.9) (6). Tubulin was polymerized for 1 h at 37 °C,  $G\alpha_s^{Q227L}$  (exchanged into G-PEM buffer using a Microcon spin concentrator) was added to microtubules for 1 h at 37 °C, and the microtubules were separated from soluble tubulin at 100,000  $\times g$  for 1 h at 37 °C (Beckman TL-100). Final reaction volume, including  $G\alpha_s$ , was 20  $\mu$ l. The pelleted protein was resuspended in 20  $\mu$ l of water at 4 °C. Two  $\mu$ l of each fraction were run on a 10% SDS-polyacrylamide gel (125 V, 2 h), followed by Coomassie Blue staining, to determine the relative mass of polymerized versus soluble tubulin.

**Microtubule Polymer Mass Concentration Response Curves**—Purified tubulin (23  $\mu$ M) was incubated for 1 h with  $G\alpha_s^{QL}$  (0.1–10  $\mu$ M) in the presence of 1 mM GTP in PEM buffer at 30 °C. Polymerization was initiated with microtubule seeds prepared from purified tubulin, 20% DMSO, and 10%

glycerol by incubating the mixture at 30 °C for 30 min and shearing the polymers formed through a 25-gauge needle. The ratio of seeds to tubulin was 1:6, and the final DMSO and glycerol concentrations were 3.3 and 1.7%, respectively. The polymers formed were then separated from solvent by centrifugation at  $35,000 \times g$  for 1 h at 30 °C. The microtubule pellets were depolymerized at 0 °C overnight, and the protein concentration was determined by the method of Bradford using BSA as the standard (20).

**Microtubule Dynamics by Video Microscopy**—Purified bovine brain tubulin (15  $\mu\text{M}$ ) was assembled onto sea urchin (*Strongylocentrotus purpuratus*) axonemes in PMEM buffer (87 mM PIPES, 36 mM MES, 1 mM EGTA, and 2 mM  $\text{MgCl}_2$ , pH 6.8) in the presence of 2 mM GTP. The reaction mixture was incubated at 30 °C for 40 min in the presence or absence of different concentrations of  $G\alpha_s^{\text{QL}}$ ,  $G\alpha_s^{\text{GtL/QL}}$ , peptide P3, or the control peptide  $G\alpha_t$ . Tracking of microtubule plus-ends was carried out at 30 °C by video-enhanced differential interference contrast microscopy using an Olympus IX71 inverted microscope with a  $\times 100$  (numerical aperture = 1.4) oil immersion objective (21). The end of an axoneme that possessed more, faster growing, and longer microtubules than the opposite end was designated as the plus-end as described previously (21). The real-time, 10-min videos were analyzed using Real Time Measurement (RTM II) software, and the data were collected using IgorPro (MediaCybernetics, Bethesda, MD). Microtubules were considered to be growing if they increased in length  $>0.3 \mu\text{m}$  at a rate of  $\geq 0.3 \mu\text{m}/\text{min}$ . Shortening events were identified by a  $>1\text{-}\mu\text{m}$  length change at a rate of  $\geq 2 \mu\text{m}/\text{min}$ . We calculated the catastrophe frequency by dividing the total number of catastrophes (transitions to shortening) by the time the microtubules were growing and in the attenuated state. The rescue (transition from shortening to growing) frequency was calculated as the total number of rescue events divided by the total time shortening. Dynamicity was calculated as the sum of the total growth length and the total shortening length divided by the total time (22).

**Molecular Modeling**—A previously published model of the  $G\alpha_s$ -tubulin complex structure, based upon a  $G\alpha_s$  crystal structure and the structure of tubulin by electron crystallography, was refined to optimize side chain orientations using SCWRL 3.0 (13, 23, 24). To determine the structure of the  $G\alpha_s^{\text{GtL/QL}}$ -tubulin complex, the  $G\alpha_s$  primary sequence was changed to corresponding  $G\alpha_t$  residues in the  $\alpha 3$ – $\beta 5$  region using an established method (25). Specifically, Modeler 9.1 (Andrej Sali, University of California, San Francisco, CA) was used to replace the residues in  $G\alpha_s$  with the corresponding  $G\alpha_t$  residues, using the “automodel” function. Likely structures (120 structures) were generated, and the lowest energy structure was used for further analysis. All structures had very similar peptide backbones on a ribbon diagram. Side chain orientation on the lowest energy complex were optimized using SCWRL version 3.0 (Roland Dunbrak, Fox Chase Cancer Center, Philadelphia, PA), followed by Amber 9.0 (Scripps Institute, La Jolla, CA) with the “all atom energy minimization” protocol for 80 steps. To permit comparison between the  $G\alpha_s^{\text{WT}}$ -tubulin and  $G\alpha_s^{\text{GtL/QL}}$  models, the  $G\alpha_s^{\text{WT}}$  model was refined using SCWRL version 3.0.

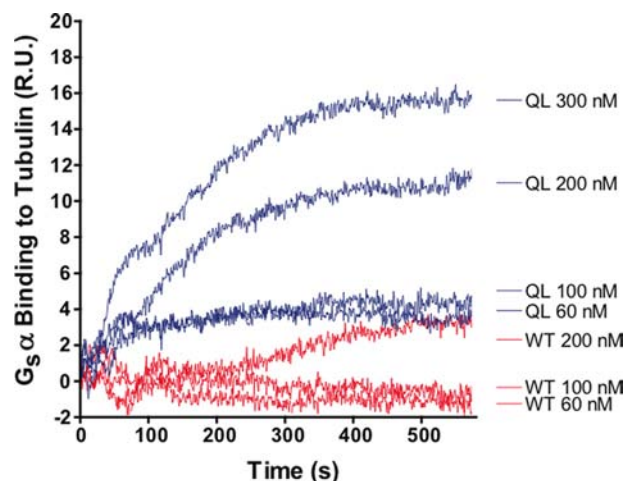


**FIGURE 1. Active  $G\alpha_s$ -GTP but not inactive  $G\alpha_s$ -GDP binds to tubulin.**  $G\alpha_s^{\text{WT}}$ -GDP (red) and  $G\alpha_s^{\text{QL}}$ -GTP (blue) were allowed to bind immobilized tubulin for 10 min. Binding was analyzed by surface plasmon resonance. Active  $G\alpha_s$ -GTP reached equilibrium in 300–400 s, whereas inactive  $G\alpha_s$ -GDP showed weak and inefficient binding to tubulin.  $k_{\text{on}} = 5 \times 10^4 \text{ M}^{-1} \text{ s}^{-1}$ ,  $k_{\text{off}} = 5 \times 10^{-3} \text{ s}^{-1}$ , and  $K_D = 100 \text{ nM}$ . This suggests that the active form of  $G\alpha_s$  is preferred for tubulin binding. Curves are representative of two independent experiments. R.U., resonance units.

**Statistical Analysis**—All data were analyzed using Prism 4.0 (GraphPad Software), with  $p < 0.05$  being considered significant. Significance tests were performed as indicated. All error bars reflect S.E. unless otherwise specified, and dashed lines indicate 95% confidence intervals for best fit curves.

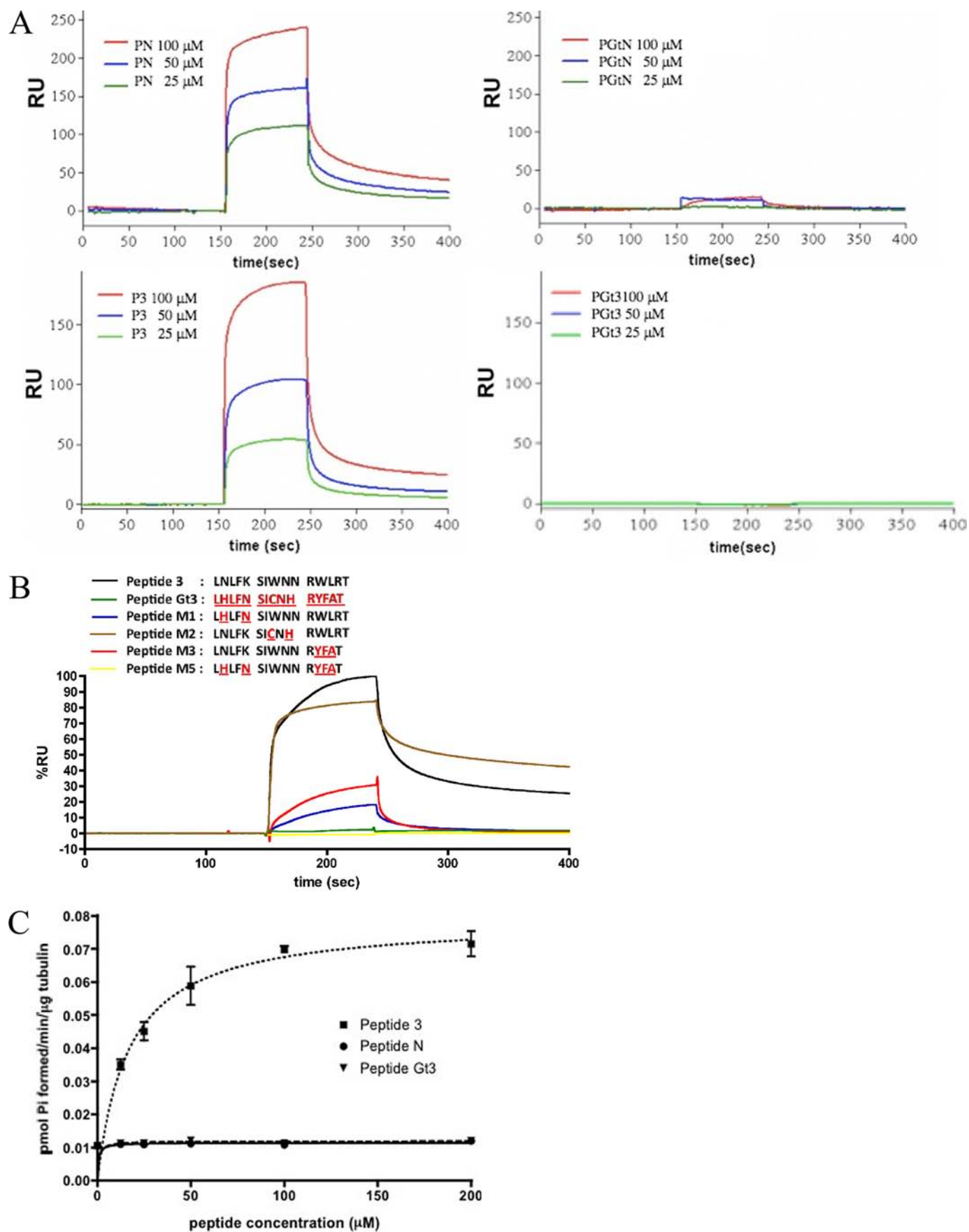
## RESULTS

**Binding and Kinetics of  $G\alpha_s$ -Tubulin Complexes**—Functional  $G\alpha_s$ -tubulin interactions promote neurite or process outgrowth in PC-12 pheochromocytoma cells and epithelial cells (6). The  $G\alpha_s$ -tubulin interaction requires  $G\alpha_s$  to be in the active (GTP-bound) form. Therefore, active  $G\alpha_s$  was generated using the Q227L mutation ( $G\alpha_s^{\text{QL}}$ ), which remains constitutively bound to GTP because it cannot hydrolyze the nucleotide (26). Inactive  $G\alpha_s$ -GDP, used as a control, was generated by promoting the hydrolysis of GTP on wild-type  $G\alpha_s$  by incubation with 5 mM  $\text{MgCl}_2$  for 1 h at 37 °C. The affinity and kinetics of the  $G\alpha_s$ -tubulin interaction were determined by surface plasmon resonance spectroscopy (BIAcore, SPR). Active  $G\alpha_s^{\text{QL}}$ -GTP bound tubulin with  $k_{\text{on}} = 5 \times 10^4 \text{ M}^{-1} \text{ s}^{-1}$ ,  $k_{\text{off}} = 5 \times 10^{-3} \text{ s}^{-1}$ , and an affinity of 100 nM (Fig. 1). The results are concordant with previous studies and indicate that  $G\alpha_s$  must be active in order to bind tubulin (6, 11).

Modeling of the  $G\alpha_s$ -tubulin complex reveals that  $G\alpha_s$  is located close to the nucleotide in  $\beta$ -tubulin. In particular, the  $\alpha 3$ – $\beta 5$  region of  $G\alpha_s$  is intimately involved in the interface. These results are consistent with a proteomic study using  $G\alpha_s$ -derived peptides (13), suggesting that the  $\alpha 3$ – $\beta 5$  region of  $G\alpha_s$  might be involved in the interface with tubulin.

**$G\alpha_s$  Peptides Derived from the  $\alpha 3$ – $\beta 5$  Region Bind to Tubulin**—Previous studies have indicated that the  $\alpha 3$ – $\beta 5$  region and a region near the N terminus of  $G\alpha_s$  may be the regions that bind to tubulin (13). To further understand the role of these regions in binding, 15-amino acid-long peptides cor-

## Mechanism for $G\alpha_s$ -mediated Microtubule Destabilization



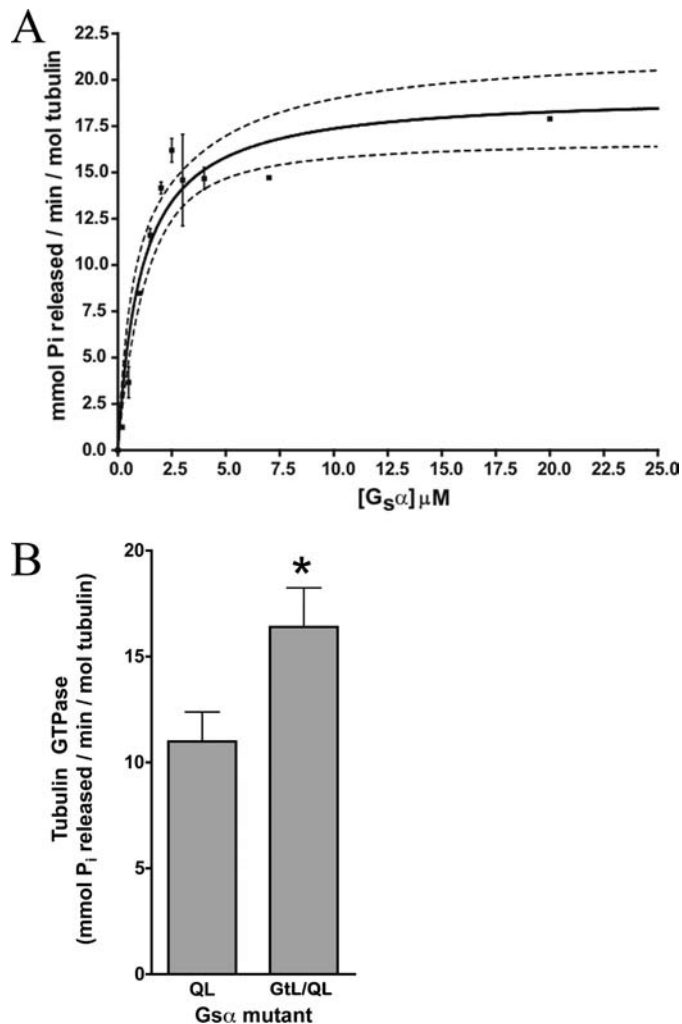


**FIGURE 3.  $G\alpha_s^{QL}$  and chimeric  $G\alpha_s^{QL}$  proteins stimulate tubulin GTPase.** A, active  $G\alpha_s$  was incubated with tubulin-GTP (200 nM) for 30 min, and the tubulin GTPase rate was determined.  $EC_{50} = 1.2 \mu M$ ,  $V_{max} = 20$  mmol of GTP hydrolyzed/min/mol of tubulin, and  $n_H = 1.0$ . Dashed lines, 95% confidence interval for a hyperbolic fit.  $n = 4$ . B, active  $G\alpha_s$ - $G\alpha_t$  chimera involving the  $\alpha 3$ - $\beta 5$  loop ( $G\alpha_s^{GtL/QL}$ ) activates tubulin GTPase. Both  $G\alpha_s$  proteins were 2  $\mu M$ .  $p < 0.01$  versus  $G\alpha_s^{QL}$ . Error bars, S.E.

responding to the  $\alpha 3$ - $\beta 5$  regions (P3) or residues 28-42 (peptide N) were synthesized (supplemental Table 2). Control peptides (peptides G $\alpha_t$ N and G $\alpha_t$ 3) were derived from  $G\alpha_t$ , which does not bind tubulin (11, 27), and corresponded to homologous regions on  $G\alpha_s$ . The affinities of all peptides for tubulin were determined. Peptide 3 (P3) bound with a  $K_D$  of 40  $\mu M$ , and peptide N displayed 10  $\mu M$  affinity (Fig. 2A), whereas none of the control ( $G\alpha_t$ -derived) peptides bound tubulin. In order to evaluate the contribution of specific residues of P3, four derivative peptides in which some residues were replaced by their  $G\alpha_t$  (transducin) homologues were evaluated for their affinity for tubulin (M1, M2, M3, and M5; Fig. 2B

**FIGURE 2.  $G\alpha_s$ -derived peptides specifically interact with tubulin.** A, sensorgrams from surface plasmon resonance analysis show the mass of indicated peptides bound to tubulin over time (in resonance units (RU)). Varying concentrations of  $G\alpha_s$ -derived N-terminal peptide (peptide N (PN)),  $G\alpha_t$ -derived N-terminal peptide (PGtN),  $G\alpha_s$ -derived  $\alpha 3$ - $\beta 5$  peptide (P3), and  $G\alpha_t$ -derived  $\alpha 3$ - $\beta 5$  peptide (PGt3) were used.  $n = 3$  experiments. B, four variants of P3 (M1, M2, M3, and M5) were synthesized by replacing  $G\alpha_s$  residues with homologous residues in transducin (indicated in red). The binding of 100  $\mu M$  peptides to immobilized tubulin is shown. C, activation of tubulin GTPase by a  $G\alpha_s$ -derived peptide (P3). P3 increased tubulin GTPase in a dose-dependent, saturable fashion.  $V_{max} = 0.070$  pmol of  $P_i$  formed/min/ $\mu g$  of tubulin, and  $EC_{50} = 24 \mu M$ . Peptide N and peptide G $\alpha_t$ 3 have no measurable effect on tubulin GTPase. All peptides are listed in supplemental Table 2.

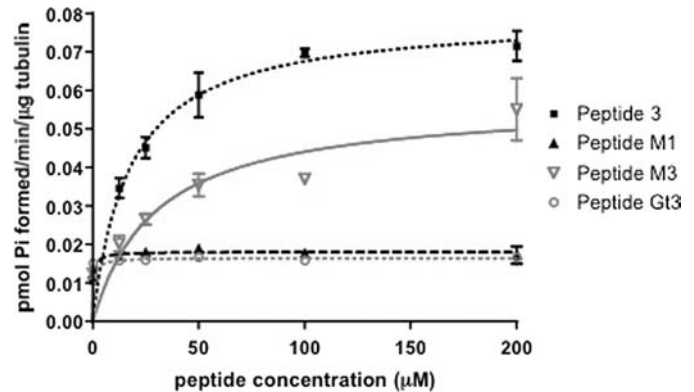


**FIGURE 4. Two peptides that bind tubulin similarly have differential effects on tubulin GTPase.** Peptides M3 and M1 bind tubulin with similar affinities. However, only peptide M3 stimulates tubulin GTPase activity ( $V_{max} = 0.057$  pmol/min/ $\mu g$  tubulin;  $EC_{50} = 29 \mu M$ ), although less efficaciously than P3 ( $V_{max} = 0.070$  pmol/min/ $\mu g$  tubulin;  $EC_{50} = 24 \mu M$ ). Error bars, S.E.

and supplemental Table 2). Peptide M2 bound tubulin with an affinity similar to P3 (45  $\mu M$ ) and much more tightly than peptides M1 ( $K_D = 373 \mu M$ ) and M3 ( $K_D = 313 \mu M$ ). Peptide M5, which differs from P3 by only 5 residues, did not bind tubulin.

**$G\alpha_s$  Activation of Tubulin GTPase Is Unaltered by Mutating the  $\alpha 3$ - $\beta 5$  Loop**—In order to determine the functional importance of the  $\alpha 3$ - $\beta 5$  loop within the context of  $G\alpha_s$ , a chimera of  $G\alpha_s$  and  $G\alpha_t$  ( $G\alpha_s^{GtL/QL}$ ) was generated, taking into consideration the fact that  $G\alpha_t$  does not bind tubulin. Specifically, the  $\alpha 3$ - $\beta 5$  loop of  $G\alpha_s$  was replaced with homologous residues from  $G\alpha_t$ . A similar approach has been used successfully to dissect the interface of  $G\alpha$  subunits with other proteins, including tubulin (13, 16, 27, 28).

$G\alpha_s^{QL}$  stimulated tubulin GTPase with an  $EC_{50}$  of 1.2  $\mu M$   $G\alpha_s$  and  $n_H = 1.0$  (Fig. 3A). This indicates non-cooperative activation of tubulin GTPase by  $G\alpha_s$  and is consistent with a 1:1 stoichiometry between the two proteins. The  $G\alpha_s^{GtL/QL}$  mutants exhibited slightly greater activation of tubulin GTPase activity compared with  $G\alpha_s^{QL}$  (16 versus 11 nmol of  $P_i$  formed/min/pmol of tubulin with 2  $\mu M$  G protein) (Fig. 3B), suggesting that although the  $\alpha 3$ - $\beta 5$  loop is involved in modulating tubulin GTPase activity, its importance within the context of the protein is diminished relative to the peptide. Note that  $G\alpha_s^{GtL/QL}$  bound tubulin similarly to parent  $G\alpha_s^{QL}$  (supplemental Fig. 2).

**$G\alpha_s$ -derived Peptides Functionally Mimic the G Protein Stimulation of Tubulin GTPase**—Next, the functional effect of  $G\alpha_s$ -derived peptides was tested. The  $\alpha 3$ - $\beta 5$ -derived peptide (P3) mimicked  $G\alpha_s$  by stimulating tubulin GTPase with an  $EC_{50}$  of 24  $\mu M$  (Fig. 2C). Peptide M2 also stimulated tubulin GTPase but with a lower potency of 47  $\mu M$  (supplemental Fig. 1). Additionally, peptide N and two peptides with portions of the  $\alpha 3$ - $\beta 5$  region from both  $G\alpha_s$  and  $G\alpha_t$  (M1 and

## Mechanism for $G\alpha_s$ -mediated Microtubule Destabilization

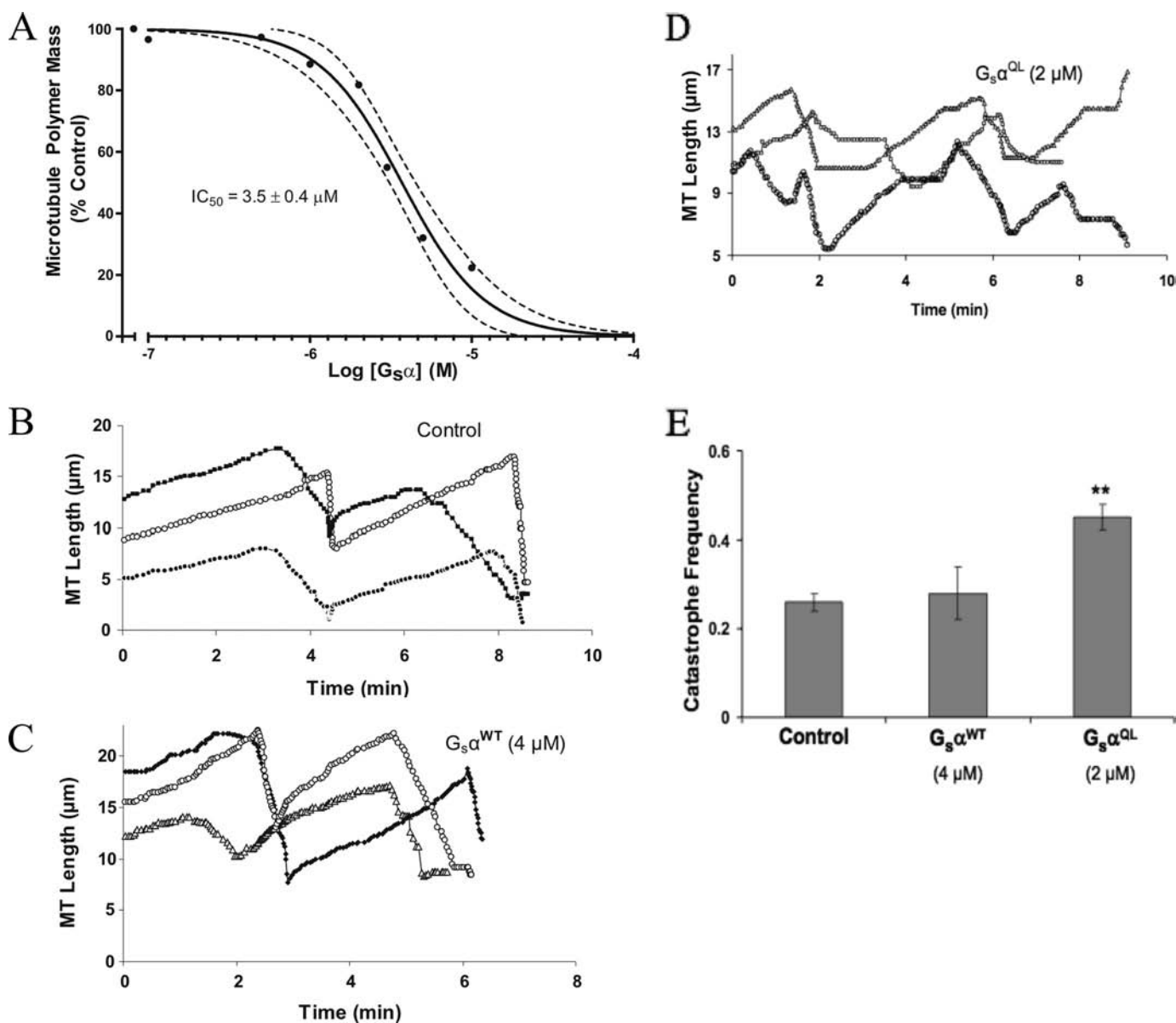


**FIGURE 5. Active  $G\alpha_s$  promotes microtubule depolymerization and increases the catastrophe frequency.** *A*, tubulin (23  $\mu M$ ) was incubated with  $G\alpha_s^{QL}$  for 1 h at 30 °C in the presence of 1 mM GTP. Microtubules were pelleted by centrifugation, and the amount of tubulin in supernatant and pellet fractions was quantified (see "Experimental Procedures").  $G\alpha_s^{QL}$  inhibited microtubule assembly with an  $IC_{50}$  of  $3.5 \pm 0.4 \mu M$  ( $n = 3$ ). *B–D*, life history plot of microtubules in the absence (*B*) or presence of inactive (*C*) or active (*D*)  $G\alpha_s$ .  $G\alpha_s$  was added to microtubules polymerized on sea urchin axoneme seeds, and the length of microtubules was determined over time (see "Experimental Procedures"). Three representative microtubules are shown in each panel. *E*, effect of inactive ( $G\alpha_s^{WT}$ ) and active ( $G\alpha_s^{QL}$ ) G proteins on the catastrophe frequency (events/min). \*\*\*,  $p < 0.001$ . Dashed lines, 95% confidence interval for best fit curves; error bars, S.E.

M6) bound to tubulin but failed to stimulate tubulin GTPase, indicating that P3 stimulates tubulin GTPase uniquely (Fig. 4 and supplemental Fig. 1). Peptide M5 does not bind tubulin and, consequently, was without effect on tubulin GTPase (supplemental Fig. 2). Thus, a peptide corresponding to the  $\alpha 3$ – $\beta 5$  region of  $G\alpha_s$  that mimics the effect of the entire  $G\alpha_s$  protein on tubulin GTPase further suggests the functional importance of this region.

*The Active Conformation of  $G\alpha_s$  Increases Microtubule Dynamic Instability*—Because  $G\alpha_s$  stimulates tubulin GTPase, it would be expected to increase the switching at microtubule ends from growth to shortening (*i.e.* to increase the catastrophe frequency). To test this prediction, the effects of  $G\alpha_s$  on

overall microtubule stability and on dynamic instability were determined.

First, the effect of active  $G\alpha_s$  on total microtubule polymer mass was determined. Purified tubulin (23  $\mu M$ ) was incubated with  $G\alpha_s^{QL}$  (0.1–10  $\mu M$ ) for 1 h at 30 °C, and microtubule pellets were separated from soluble tubulin by centrifugation (see "Experimental Procedures").  $G\alpha_s^{QL}$  destabilized microtubules in a concentration-dependent manner (Fig. 5*A*) with an  $IC_{50}$  of  $3.5 \pm 0.4 \mu M$ . This concentration is probably physiologic because  $G\alpha_s$  is delivered to microtubule ends at a high local concentration on the surface of endocytic vesicles (6, 10).

Next, the steady state dynamic instability behavior of microtubules in the presence of  $G\alpha_s$  was determined by video

TABLE 1

Effects of  $G\alpha_s^{QL}$ , and  $G\alpha_s^{GtL/QL}$  on microtubule dynamic instability

Microtubules were polymerized to steady state at the ends of axoneme seeds in the absence and presence of  $G\alpha_s^{QL}$  or  $G\alpha_s^{GtL/QL}$ , and the dynamic instability parameters were determined (see "Experimental Procedures"). 15–25 microtubules were measured for each protein concentration. Data are mean  $\pm$  S.E.

Dynamic instability parameters	Control	$G\alpha_s^{QL}$ (1 $\mu$ M)	$G\alpha_s^{QL}$ (2 $\mu$ M)	$G\alpha_s^{GtL/QL}$ (1 $\mu$ M)	$G\alpha_s^{GtL/QL}$ (2 $\mu$ M)
Growing rate ( $\mu$ m/min)	1.6 $\pm$ 0.1	2.0 $\pm$ 0.2 <sup>a</sup>	2.6 $\pm$ 0.1 <sup>b</sup>	2.6 $\pm$ 0.2 <sup>b</sup>	3.1 $\pm$ 0.3 <sup>c</sup>
Shortening rate ( $\mu$ m/min)	8.9 $\pm$ 0.7	10.6 $\pm$ 1	12.4 $\pm$ 1.3 <sup>b</sup>	12.8 $\pm$ 1 <sup>b</sup>	13.4 $\pm$ 0.8 <sup>c</sup>
Time growing (%)	39	47	35	50	43
Time shortening (%)	11	20	23	20	18
Time attenuated (%)	50	33	42	30	39
Catastrophe frequency (per min)	0.26 $\pm$ 0.02	0.45 $\pm$ 0.04 <sup>b</sup>	0.45 $\pm$ 0.02 <sup>b</sup>	0.59 $\pm$ 0.1 <sup>c</sup>	0.62 $\pm$ 0.05 <sup>c</sup>
Rescue frequency (per min)	1.42 $\pm$ 0.2	1.13 $\pm$ 0.2	0.98 $\pm$ 0.1 <sup>a</sup>	1.22 $\pm$ 0.05	1.44 $\pm$ 0.2
Dynamicity	1.44	2.05	2.35	2.83	2.94

<sup>a</sup> $p$  < 0.05 with respect to control.

<sup>b</sup> $p$  < 0.01 with respect to control.

<sup>c</sup> $p$  < 0.001 with respect to control.

microscopy.  $G\alpha_s^{QL}$  increased the growing rate, the shortening rate, and the catastrophe frequency (Fig. 5 and Table 1). In contrast,  $G\alpha_s^{WT}$  had no significant effect on any dynamics parameter, which is consistent with its weak ability to bind tubulin or to stimulate tubulin GTPase (supplemental Table 3; dynamicity was 1.44 with buffer control and 1.40 in the presence of  $G\alpha_s^{WT}$ ). Specifically,  $G\alpha_s^{QL}$  increased the growing rate by 25% (1  $\mu$ M) and 63% (2  $\mu$ M), and increased the catastrophe frequency by 73%. The dynamicity was enhanced by 42% (1  $\mu$ M) and 63% (2  $\mu$ M). Notably, 1  $\mu$ M  $G\alpha_s$  caused minimal depolymerization but increased microtubule dynamicity by 42% and nearly doubled the catastrophe frequency, indicating that the primary function of  $G\alpha_s$  may be to increase microtubule dynamics rather than to affect microtubule polymer mass.

Consistent with its effects on tubulin GTPase,  $G\alpha_s^{GtL/QL}$  promoted microtubule depolymerization more strongly than  $G\alpha_s^{QL}$  (1.6-fold difference; Fig. 6A). Moreover, this mutant increased microtubule dynamics more strongly than  $G\alpha_s^{QL}$ . For example, whereas 2  $\mu$ M  $G\alpha_s$  increased the growing rate, the catastrophe frequency, and the dynamicity by 63, 73, and 63%, respectively, the same concentration of  $G\alpha_s^{GtL/QL}$  increased these parameters by 94, 138, and 104%, respectively (Fig. 6B and Table 1).

*$G\alpha_s$ -derived Peptides Increase Microtubule Dynamics*—We also determined the effects of the  $\alpha 3$ – $\beta 5$ -derived peptide (peptide P3) on dynamic instability. The peptide also increased microtubule dynamics but required concentrations higher than those required for the full-length proteins. Specifically, whereas 4  $\mu$ M P3 did not have any significant effect on dynamic instability, 10 and 20  $\mu$ M peptide P3 destabilized the microtubules significantly. For example, at 20  $\mu$ M, peptide P3 increased the growing rate by 63% and the catastrophe frequency by 188%. (Fig. 7 and Table 2). The overall dynamicity was increased by 68% compared with the control. These results suggest that  $\alpha 3$ – $\beta 5$ -derived peptide P3 mimics the effect of full-length  $G\alpha_s$  predominantly by increasing the catastrophe frequency.

## DISCUSSION

The data presented in this report suggest a model for the action of  $G\alpha_s$  on microtubules. We have previously reported that in response to agonist stimulation,  $G\alpha_s$  moves from the plasma membrane to the cytosol and associates with microtu-

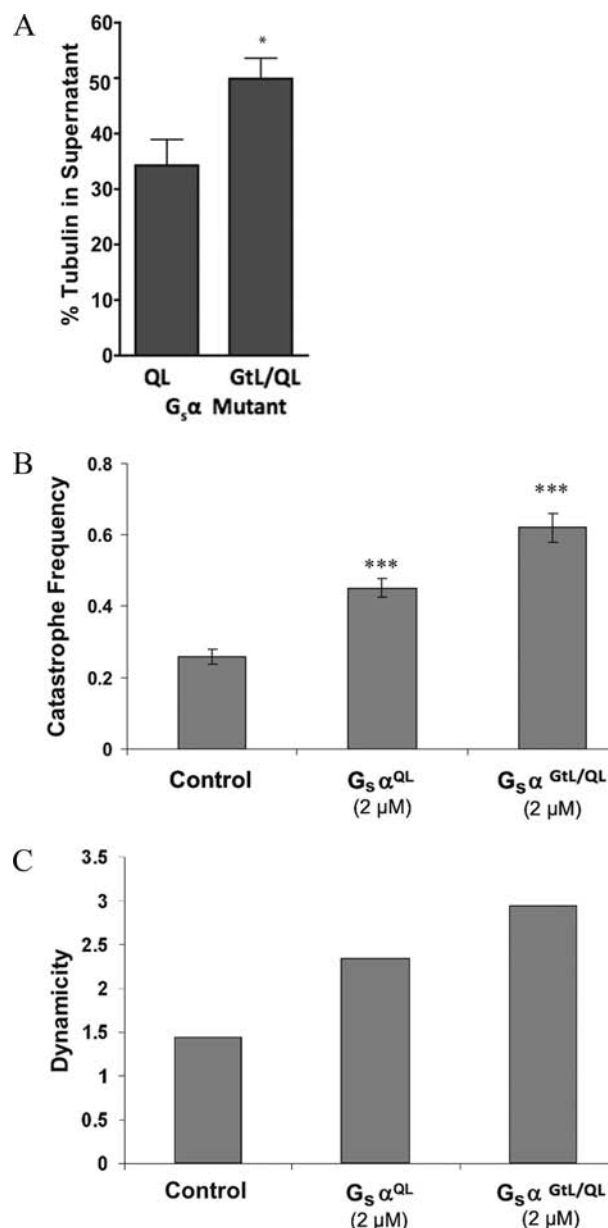


FIGURE 6.  $G\alpha_s^{GtL/QL}$  promotes microtubule depolymerization and dynamic instability to a greater extent than  $G\alpha_s^{QL}$ . A, 15  $\mu$ M  $G\alpha_s^{QL}$  and 15  $\mu$ M  $G\alpha_s^{GtL/QL}$  (mutation only in the  $\alpha 3$ – $\beta 5$  loop) were added to microtubules (15  $\mu$ M) at 37  $^{\circ}$ C for 60 min in the presence of 200  $\mu$ M GTP.  $G\alpha_s^{GtL/QL}$  depolymerized microtubules to a greater extent than  $G\alpha_s^{QL}$ .  $G\alpha_s^{GtL/QL}$  increased the catastrophe frequency (events/min; error bars represent S.E.) (B) and dynamicity (C). \*,  $p$  < 0.01; \*\*\*,  $p$  < 0.001.

## Mechanism for $G\alpha_s$ -mediated Microtubule Destabilization

bule plus-ends (6, 10). We propose that active  $G\alpha_s$  both promotes hydrolysis of GTP on tubulin and sequesters the newly released tubulin-GDP, resulting in increased microtubule dynamics. This process is probably terminated by the autohydrolysis of GTP on  $G\alpha_s$ . First, we show here that  $G\alpha_s$  must be in an active conformation ( $G\alpha_s$ -GTP) in order to bind tubulin, to stimulate tubulin GTPase, and to increase microtubule dynamic instability (Fig. 1). The 1:1 interaction of  $G\alpha_s$  with tubulin and 1  $\mu\text{M}$  potency of  $G\alpha_s$  for tubulin GTPase (and 3  $\mu\text{M}$  for microtubule depolymerization) support a model whereby  $G\alpha_s$  is delivered to intracellular microtubule plus-ends on the cytosolic surface of lipid raft-derived vesicle

membranes (10, 29, 30). The intracellular concentration of tubulin is in the micromolar range, and  $G\alpha_s$  targets microtubules upon internalization (6).

Our results also show that 1  $\mu\text{M}$   $G\alpha_s$  causes a 2-fold increase in the catastrophe frequency with minimal depolymerization of the microtubules (Figs. 5 and 6 and Table 1), suggesting that the primary effect of  $G\alpha_s$  is on microtubule dynamics rather than on the mass of assembled polymer. This is consistent with neuronal outgrowth being a dynamic process involving both extension and retraction (31). In addition,  $G\alpha_s$  has a much higher affinity for tubulin (100 nM) than potency for tubulin GTPase (1  $\mu\text{M}$ ) (32, 33). We suggest that  $G\alpha_s$  sequesters tubulin-GDP to prevent reassociation with microtubules after nucleotide exchange using cytosolic GTP. Indeed,  $G\alpha_s$  binds to both tubulin-GDP and tubulin-GTP (6).

Structurally, the  $\alpha 3$ - $\beta 5$  region of  $G\alpha_s$  appears to be the principal region through which  $G\alpha_s$  mediates its activation of tubulin GTPase. Computational modeling data place this region near the hydrolyzable GTP on tubulin. Mutagenesis of this region alters  $G\alpha_s$  stimulation of tubulin GTPase and microtubule dynamics. Furthermore, a peptide corresponding to this region mimics the effects of  $G\alpha_s$  on tubulin GTPase, microtubule stability, and dynamics (Figs. 2, 4, and 7 and Table 2). The  $\alpha 3$ - $\beta 5$  region of  $G\alpha_s$  is a highly interactive surface on that molecule because it mediates  $G\alpha$  interaction with adenylyl cyclase and  $G\beta\gamma$  (34, 35). This result lends support to the idea that tubulin, like adenylyl cyclase, is an effector for  $G\alpha_s$ .

Perhaps counterintuitively, the  $G\alpha_s^{G1L/QL}$  chimera stimulates tubulin GTPase and increases microtubule dynamic instability to a slightly greater extent than  $G\alpha_s^{QL}$  (Figs. 3 and 6 and Table 1). Molecular modeling studies suggest that this chimera undergoes conformational changes that may be permissive for increased tubulin GTPase (Fig. 8). It does appear that the  $\alpha 3$  helix, loop, and  $\beta 5$  sheet together are crucial for getting the peptide or protein into position. Consistent with the peptide data in this paper, mutation of the two tryptophan residues in the  $\alpha 3\beta 5$  loop blocked  $G\alpha_s$ /adenylyl cyclase activation by  $\alpha 3\beta 5$  region peptides (36). Grishina and Berlot (37) substituted the  $\alpha 3\beta 5$  region from  $G_{12}$  into  $G\alpha_s$  and found that AC activation was blocked. Thus, it appears that the  $\alpha 3\beta 5$  region may be more important than the loop itself but that clear conformational distinctions must be drawn between the proteins and peptides derived from those proteins. Ultimately, rigorous evaluation of this will require crystallization of  $G\alpha_s$ -

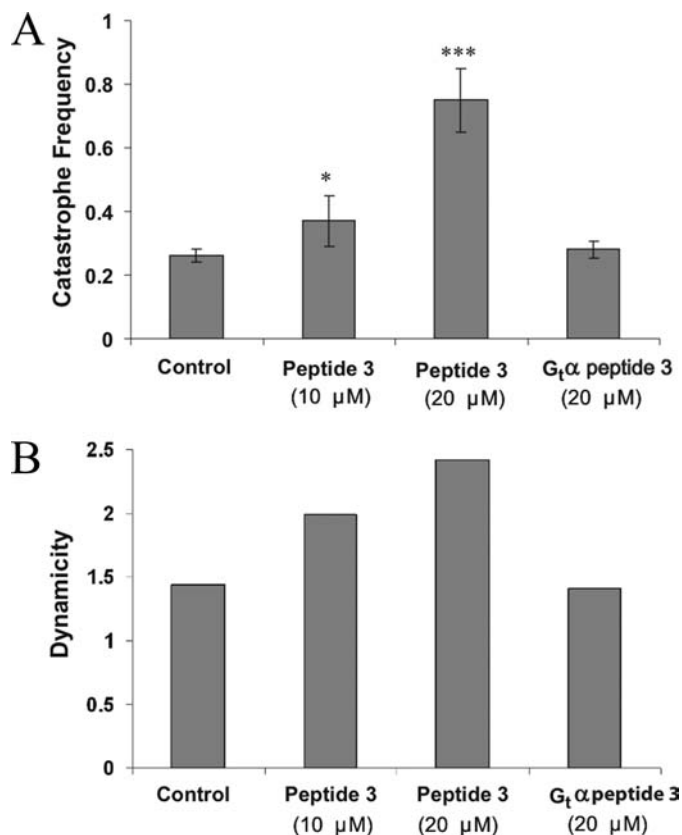


FIGURE 7. A peptide derived from the  $\alpha 3$ - $\beta 5$  region of  $G\alpha_s$  (P3) mimics  $G\alpha_s$  protein in increasing the catastrophe frequency and dynamicity of microtubules. A, 20  $\mu\text{M}$   $G\alpha_s$  peptide P3 increases the catastrophe frequency (events/min) by 188%, whereas the homologous  $G\alpha_t$  peptide ( $PG_13$ ) had no effect. Error bars, S.E. B, in the presence of  $G\alpha_s$  P3, the overall dynamicity increased 68% compared with the control (tubulin alone).  $G\alpha_t$  P3 has no effect on dynamicity. \*,  $p < 0.01$ ; \*\*\*,  $p < 0.001$ .

TABLE 2

### Effects of peptides on microtubule dynamic instability

Tubulin was polymerized to steady state with axoneme seeds in the absence and presence of P3 or control peptide ( $PG_13$ ), and the dynamic instability parameters were determined (see "Experimental Procedures"). 15–25 microtubules were measured for each peptide concentration. Data are mean  $\pm$  S.E.

Dynamic instability parameters	Control	P3 Peptide (4 $\mu\text{M}$ )	P3 Peptide (10 $\mu\text{M}$ )	P3 Peptide (20 $\mu\text{M}$ )	$PG_13$ Peptide (20 $\mu\text{M}$ )
Growing rate ( $\mu\text{m}/\text{min}$ )	1.6 $\pm$ 0.1	1.7 $\pm$ 0.2	1.95 $\pm$ 0.2 <sup>a</sup>	2.6 $\pm$ 0.3 <sup>b</sup>	1.5 $\pm$ 0.2
Shortening rate ( $\mu\text{m}/\text{min}$ )	8.9 $\pm$ 0.7	9.6 $\pm$ 0.9	12.5 $\pm$ 1 <sup>b</sup>	13.6 $\pm$ 1 <sup>b</sup>	9.2 $\pm$ 0.7
Time growing (%)	39	26.2	39.6	21.5	42
Time shortening (%)	11	10.2	11.2	15.6	10.4
Time attenuated (%)	50	63.6	49.2	62.9	47.6
Catastrophe frequency (per min)	0.26 $\pm$ 0.02	0.26 $\pm$ 0.02	0.37 $\pm$ 0.01 <sup>a</sup>	0.75 $\pm$ 0.1 <sup>c</sup>	0.28 $\pm$ 0.03
Rescue frequency (per min)	1.42 $\pm$ 0.2	1.40 $\pm$ 0.2	1.39 $\pm$ 0.2	1.36 $\pm$ 0.3	1.32 $\pm$ 0.4
Dynamicity	1.44	1.38	1.99	2.42	1.41

<sup>a</sup> $p < 0.05$  as observed in a  $t$  test with respect to control.

<sup>b</sup> $p < 0.01$  as observed in a  $t$  test with respect to control.

<sup>c</sup> $p < 0.001$  as observed in a  $t$  test with respect to control.

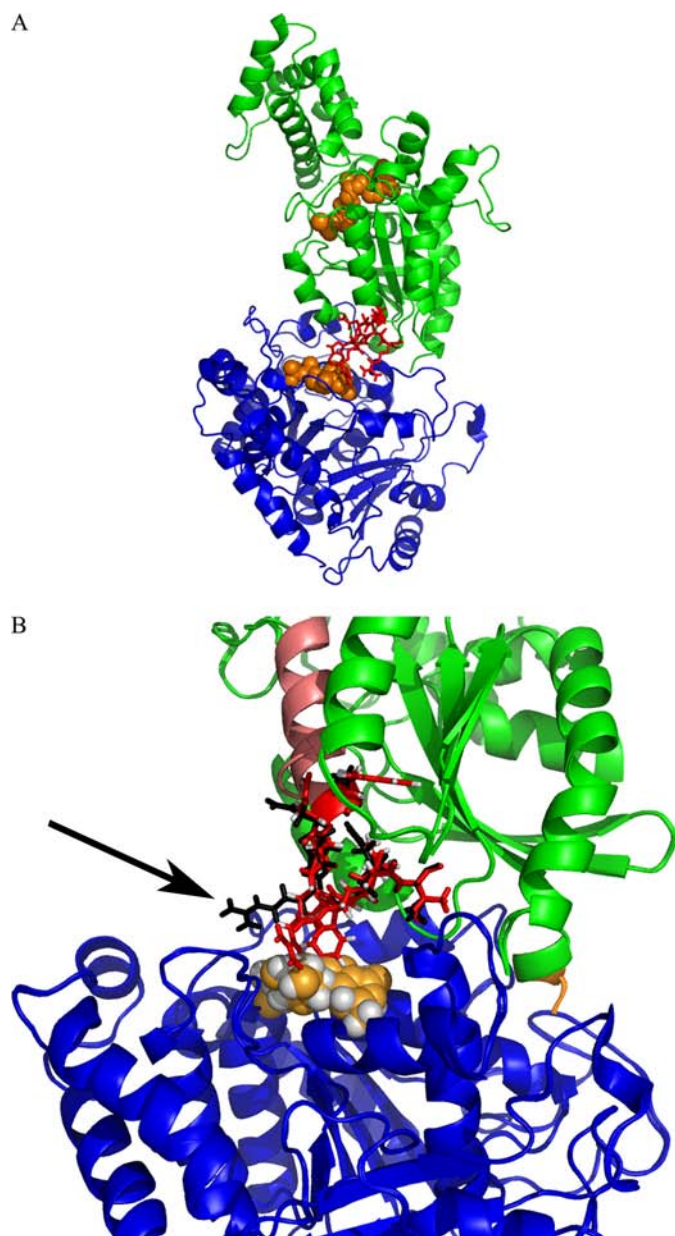


**FIGURE 8. Molecular model of  $G\alpha_s$ -GTP $\gamma$ S (guanosine 5'-(3-O-thio)triphosphate) complexed with tubulin-GDP.** *A*, molecular modeling (described under "Experimental Procedures") was used to visualize the  $G\alpha_s$ -GTP-tubulin-GDP complex. *Blue*, tubulin; *green*,  $G\alpha_s$ . The GDP on tubulin (*orange spheres*) is located in close proximity to  $G\alpha_s$ . Note the  $\alpha$ 3- $\beta$ 5 loop (*red*) on  $G\alpha_s$  is in close proximity to tubulin. *B*, the  $G\alpha_s$ -tubulin interface is expanded in this model, and interacting residues are shown in *red* (WT) or *black* (GtL/QL). The GDP on tubulin is shown in *orange*. The  $\alpha$ 3 helix is shown in *pink* and is located far from the  $G\alpha_s$ -tubulin interface. This model suggests that, in  $G\alpha_s^{\text{GtL/QL}}$ , the indicated (*black arrow*) positively charged Arg residue undergoes a positional change that decreases steric hindrance with GTP on tubulin and may additionally position to better abstract the terminal phosphate (note that nucleotide is still shown as GDP).

tubulin complexes to allow for subnanometer resolution of the structure.

We have also developed short peptides (P3, M2, and M3) that mimic the effects of  $G\alpha_s$  on tubulin and microtubules (Figs. 2, 4, and 7 and Table 2). Introduction of these peptides should be useful tools to probe  $G\alpha_s$ -tubulin interactions in living cells. Peptides have been successfully used to study G protein signaling in striatal membranes as well as in intact

cells, even at high micromolar concentrations (38, 39). The specificity of effects in cells can be assessed both by using inactive  $G\alpha_s$  peptides that bind tubulin (M1, M6, and PN) and homologous peptides that do not bind tubulin (PG<sub>t</sub> and P5) (Figs. 2, 4, and 7 and Table 2). Peptides (or peptide mimetics) that target the  $G\alpha_s$ /tubulin interface might be of therapeutic usefulness to promote neurite outgrowth and synaptogenesis.

Neurotransmitter (activity)-dependent neuronal remodeling plays a role during development and antidepressant response, and involves alterations in both G protein signaling and microtubule dynamic instability (31, 40–42). Indeed, plastic regions, such as immature dendritic spines, contain highly dynamic microtubules (4, 43). We have recently shown that  $G\alpha_s$ , even in the absence of cAMP signaling, modulates microtubule stability and promotes neurite outgrowth in cells (6). These processes may occur via a direct interaction of  $G\alpha_s$  with microtubules. The data presented in this report suggest a mechanism for neurotransmitter-induced remodeling of the cytoskeleton and raise the possibility that small molecule probes can be generated to manipulate this process.

*Acknowledgments*—We thank Aarti Sharma for help with designing and preparing G protein mutants and Herb Miller for preparing bovine brain tubulin.

## REFERENCES

- Lopus, M., Yenjerla, M., and Wilson, L. (2009) *Wiley Encyclopedia of Chemical Biology* (Begley, T. P., ed) Vol. 3, pp. 153–160, John Wiley & Sons, Inc., New York
- Conde, C., and Caceres, A. (2009) *Nat. Rev. Neurosci.* **10**, 319–332
- Suter, D. M., Schaefer, A. W., and Forscher, P. (2004) *Curr. Biol.* **14**, 1194–1199
- Jaworski, J., Kapitein, L. C., Gouveia, S. M., Dortland, B. R., Wulf, P. S., Grigoriev, I., Camera, P., Spangler, S. A., Di Stefano, P., Demmers, J., Krugers, H., Defilippi, P., Akhmanova, A., and Hoogenraad, C. C. (2009) *Neuron* **61**, 85–100
- van Rossum, D., Kuhse, J., and Betz, H. (1999) *J. Neurochem.* **72**, 962–973
- Yu, J. Z., Dave, R. H., Allen, J. A., Sarma, T., and Rasenick, M. M. (2009) *J. Biol. Chem.* **284**, 10462–10472
- Roychowdhury, S., and Rasenick, M. M. (2008) *FEBS J.* **275**, 4654–4663
- Roychowdhury, S., Panda, D., Wilson, L., and Rasenick, M. M. (1999) *J. Biol. Chem.* **274**, 13485–13490
- Piao, X., Hill, R. S., Bodell, A., Chang, B. S., Basel-Vanagaite, L., Straussberg, R., Dobyns, W. B., Qasrawi, B., Winter, R. M., Innes, A. M., Voit, T., Ross, M. E., Michaud, J. L., Descarie, J. C., Barkovich, A. J., and Walsh, C. A. (2004) *Science* **303**, 2033–2036
- Allen, J. A., Yu, J. Z., Donati, R. J., and Rasenick, M. M. (2005) *Mol. Pharmacol.* **67**, 1493–1504
- Wang, N., Yan, K., and Rasenick, M. M. (1990) *J. Biol. Chem.* **265**, 1239–1242
- Yan, K., Greene, E., Belga, F., and Rasenick, M. M. (1996) *J. Neurochem.* **66**, 1489–1495
- Layden, B. T., Saengsawang, W., Donati, R. J., Yang, S., Mulhearn, D. C., Johnson, M. E., and Rasenick, M. M. (2008) *Biochim. Biophys. Acta* **1783**, 964–973
- Linder, M. E., Ewald, D. A., Miller, R. J., and Gilman, A. G. (1990) *J. Biol. Chem.* **265**, 8243–8251
- Guo, L. W., Assadi-Porter, F. M., Grant, J. E., Wu, H., Markley, J. L., and Ruoho, A. E. (2007) *Protein Expr. Purif.* **51**, 187–197
- Skiba, N. P., Thomas, T. O., and Hamm, H. E. (2000) *Methods Enzymol.* **315**, 502–524
- Murphy, D. B. (1982) *Methods Cell Biol.* **24**, 31–49

## Mechanism for $G\alpha_s$ -mediated Microtubule Destabilization

18. Miller, H. P., and Wilson, L. (2010) *Methods Cell Biol.* **95**, 3–15
19. Mejillano, M. R., Shivanna, B. D., and Himes, R. H. (1996) *Arch. Biochem. Biophys.* **336**, 130–138
20. Yenjerla, M., LaPointe, N. E., Lopus, M., Cox, C., Jordan, M. A., Feinstein, S. C., and Wilson, L. (2010) *J. Alzheimers Dis.* **19**, 1377–1386
21. Yenjerla, M., Lopus, M., and Wilson, L. (2010) *Methods Cell Biol.* **95**, 189–206
22. Lopus, M., Oroudjev, E., Wilson, L., Wilhelm, S., Widdison, W., Chari, R., and Jordan, M. A. (2010) *Mol. Cancer Ther.* **9**, 2689–2699
23. Sunahara, R. K., Tesmer, J. J., Gilman, A. G., and Sprang, S. R. (1997) *Science* **278**, 1943–1947
24. Nogales, E., Whittaker, M., Milligan, R. A., and Downing, K. H. (1999) *Cell* **96**, 79–88
25. Xiang, Z. (2006) *Curr. Protein Pept. Sci.* **7**, 217–227
26. Graziano, M. P., and Gilman, A. G. (1989) *J. Biol. Chem.* **264**, 15475–15482
27. Chen, N. F., Yu, J. Z., Skiba, N. P., Hamm, H. E., and Rasenick, M. M. (2003) *J. Biol. Chem.* **278**, 15285–15290
28. Skiba, N. P., Bae, H., and Hamm, H. E. (1996) *J. Biol. Chem.* **271**, 413–424
29. Allen, J. A., Halverson-Tamboli, R. A., and Rasenick, M. M. (2007) *Nat. Rev. Neurosci.* **8**, 128–140
30. Dave, R. H., Saengsawang, W., Yu, J. Z., Donati, R., and Rasenick, M. M. (2009) *Neurosignals* **17**, 100–108
31. Poulain, F. E., and Sobel, A. (2010) *Mol. Cell Neurosci.* **43**, 15–32
32. Margolis, R. L., and Wilson, L. (1977) *Proc. Natl. Acad. Sci. U.S.A.* **74**, 3466–3470
33. David-Pfeuty, T., Simon, C., and Pantaloni, D. (1979) *J. Biol. Chem.* **254**, 11696–11702
34. Hamm, H. E., and Gilchrist, A. (1996) *Curr. Opin. Cell Biol.* **8**, 189–196
35. Tesmer, J. J., Sunahara, R. K., Gilman, A. G., and Sprang, S. R. (1997) *Science* **278**, 1907–1916
36. Chen, Y., Yoo, B., Lee, J. B., Weng, G., and Iyengar, R. (2001) *J. Biol. Chem.* **276**, 45751–45754
37. Grishina, G., and Berlot, C. H. (2000) *Mol. Pharmacol.* **57**, 1081–1092
38. Rasenick, M. M., Watanabe, M., Lazarevic, M. B., Hatta, S., and Hamm, H. E. (1994) *J. Biol. Chem.* **269**, 21519–21525
39. Smrcka, A. V., Kichik, N., Tarragó, T., Burroughs, M., Park, M. S., Itoga, N. K., Stern, H. A., Willardson, B. M., and Giralto, E. (2010) *Proc. Natl. Acad. Sci. U.S.A.* **107**, 639–644
40. Bianchi, M., Shah, A. J., Fone, K. C., Atkins, A. R., Dawson, L. A., Heidebreder, C. A., Hows, M. E., Hagan, J. J., and Marsden, C. A. (2009) *Synapse* **63**, 359–364
41. Lim, S. S., Sammak, P. J., and Borisy, G. G. (1989) *J. Cell Biol.* **109**, 253–263
42. Donati, R. J., and Rasenick, M. M. (2005) *Neuropsychopharmacology* **30**, 1238–1245
43. Hu, X., Viesselmann, C., Nam, S., Merriam, E., and Dent, E. W. (2008) *J. Neurosci.* **28**, 13094–13105